Investigation of the electronic structure of Ni by angle-resolved uv photoelectron spectroscopy

H. Mårtensson and P. O. Nilsson
Department of Physics, Chalmers University of Technology, S-412 96 Göteborg, Sweden
(Received 10 January 1984)

The band structure of Ni has been determined from angle-resolved uv photoelectron spectra, mainly by exploiting the dispersion of direct-transition peaks as the emission angle is changed. Starting from energy-coincidence-determined band-structure points and critical-point values from synchrotron-radiation investigations in the literature, the parameters of a combined interpolation scheme were systematically fitted to give good overall agreement with our experimental data. The resulting semiempirical band structure is characterized by a d-band narrowing of about 30%, in good agreement with several earlier investigations. For specific $\vec{k}$ points, small deviations from the earlier results were observed. The analysis is less dependent on assumptions concerning the final-state dispersion and the presented measurements are largely complementary to the earlier ones.

I. INTRODUCTION

The electronic structure of solid Ni has drawn considerable attention during the last decade. In the beginning of the 1970s it was reported[1–3] that the valence-band width as measured by photoelectron spectroscopy was smaller than that obtained from ordinary band calculations. Later a satellite structure was observed[4,5] below the valence band at about 6-eV binding energy relative to the Fermi energy. These findings were confirmed by other authors, see, e.g., Refs. 6—11. The satellite was also observed in core states but that phenomenon will not be discussed here. Other deviations from the one-electron band model have also been reported, in particular a reduced exchange splitting.[6,7,9]

The 6-eV satellite has been given different interpretations.[5,12–20] Although the details do not yet seem to be established,[20] the common opinion is that the excitation should be attributed to a many-body phenomenon rather than to a band effect.[9] Some authors have, however, not been fully convinced by this standpoint. Smith *et al.*[4] left the question open while Kleinman[21] and Kleinman and Mednick[22] favored an interband transition as the origin of the satellite. Kanski *et al.*[23] calculated photoelectron spectra from Ni(100) using a one-electron potential. Their results reproduced the behavior of the experimental spectra in the sense that a peak was found at 5-eV binding energy (6 eV experimentally) which resonates at 67-eV photon energy (67 eV experimentally). The $3p$ core level of Ni also occurs at this energy, but it should be noted that no contribution from this was included in the calculations.

Instead, the theoretical resonance was traced to originate from an interband transition at the Brillouin-zone boundary.[23,24] Since the corresponding resonance occurs in other noble and transition metals as well, both theoretically and experimentally,[25–27] it was tempting to suggest that the same mechanism is active in Ni. The main conclusion to be drawn from the work by Kanski *et al.* is that interband transitions show resonant behavior like that observed for the satellite. This is, for instance, true for the main part of the Ni valence band. The phenomenon is thus of great importance when normalizing peak amplitudes (e.g., the intensity of the satellite peak) as a function of photon energy.

Existence of a many-body satellite implies a narrowing of the valence band.[12] This phenomenon has also been questioned by some authors.[21,22,28] Anisinov *et al.*,[28] for instance, find that the excitation effect on the Ni band structure is merely a rigid shift upwards of the d band due to relaxation. Other studies[6,7,9] suggest, on the other hand, a narrowing of the upper part of the valence band.

Critical analysis of the photoemission data presented in the literature may pose some questions. So, for instance, the free-electron parabola used in Ref. 7 for the photoelectron final state was adjusted to an observed critical point. The position of the observed critical point can, however, be different from the band-structure energy due to damping mechanisms.[29]

In order to solve some of the controversies discussed above we have tried to determine accurately the band structure of Ni, as observed in uv photoelectron spectroscopy, without relying strongly on any assumptions or calculations. Thereby we have made use of the "energy-coincidence method"[30] to fix the energy bands absolutely in a number of points in the reciprocal space. An interpolation scheme was then fitted to these points and adjusted to give good overall agreement with all the photoemission data. Data from earlier measurements[7,9] were used in the initial stage of this procedure, but the final results are largely complementary to these earlier data. Very fine details such as exchange splitting, the shape of Fermi surface, etc., are outside the scope of the present work.

II. EXPERIMENTAL PROCEDURES

Three Ni single crystals were cut along the (111), (110), and (100) faces, respectively, and oriented to an accuracy of $\sim 1°$. The surfaces were polished mechanically and the (100) surface was in addition electrochemically polished. In the UHV chamber the samples were further cleaned by repeated cycles of ion sputtering and annealing at

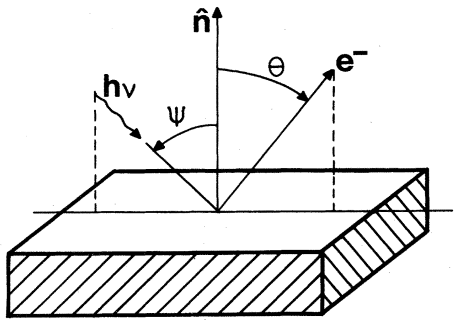

FIG. 1. Experimental configuration: $\hat{n}$, surface normal; $h\nu$, incident photons; e^-, emitted electrons.

600—800 K. The surface structure and azimuthal orientation was checked by means of low-energy electron diffraction (LEED).

The samples which were only mechanically polished required a larger number of sputtering and annealing cycles than those that were electrochemically polished in order to produce sharp LEED patterns, but the final quality of the surfaces seemed to be comparable. Surface cleanliness could be monitored by Auger electron spectroscopy using the LEED system.

The light source was a noble-gas discharge lamp, producing unpolarized radiation. Photon energies $h\nu$=16.85, 21.22, 26.9, and 40.8 eV were used. The electron-energy analyzer was of the 127° cylindrical type, and had an energy resolution of about 0.2 eV and an acceptance cone of 3° full opening. The angles of light incidence and electron detection could be varied independently. The base pressure in the chamber was 1×10^{-10} Torr, which rose to about 5×10^{-9} Torr when the lamp was operating.

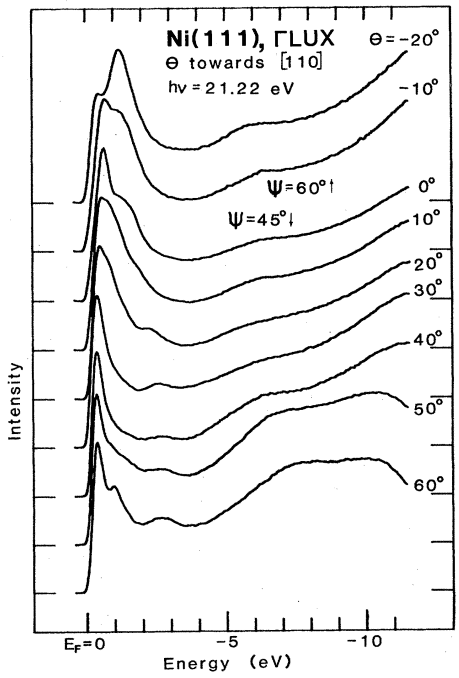

FIG. 2. EDC's from Ni(111) obtained at different emission polar angles in the Γ*LUX* mirror plane at photon energy $h\nu$=21.22 eV.

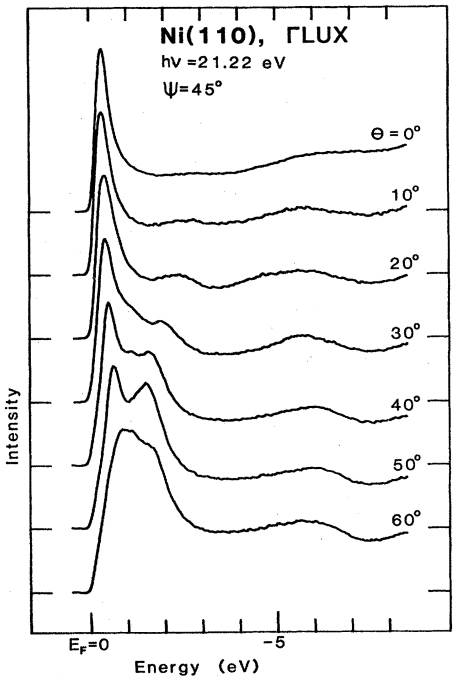

FIG. 3. Same as Fig. 2 but for Ni(110), Γ*LUX* mirror plane.

III. EXPERIMENTAL RESULTS

Energy distribution curves (EDC's) were recorded at various emission polar angles, θ, in the azimuthal mirror planes of the three surfaces. In all cases the photons were incident in the detection plane. The incidence polar angle, Ψ, defined in Fig. 1, was in general chosen to be 45°, except for some cases where 40°, 55°, or 60° were used due to experimental circumstances (geometrical limitations or in order to avoid light reflection into the analyzer). As the positions of the direct-transition peaks in the EDC's are not dependent on Ψ, we do not concern ourselves with it in the following.

Figures 2—5 show a selection of EDC's obtained with He I radiation ($h\nu$=21.22 eV) for the four combinations of surfaces and mirror planes investigated. The EDC's are characterized by strong emission in the region from the Fermi level (E_F) down to about 3 eV below. At about 6 eV below E_F a weak and broad structure with very little dispersion is seen. This feature will be discussed in Sec. V.

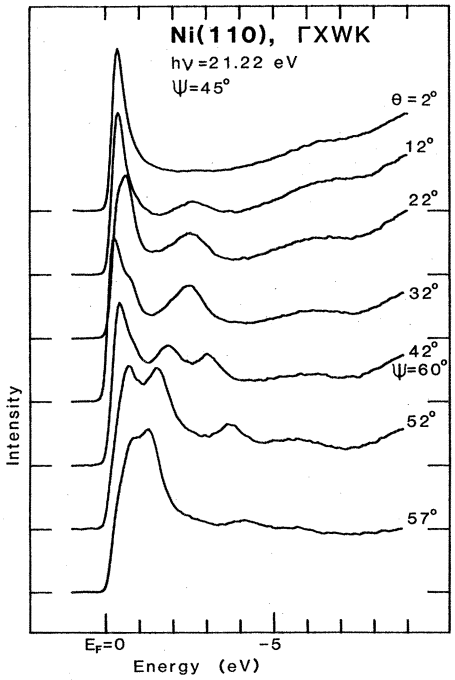

FIG. 4. Same as Fig. 2 but for Ni(110), Γ*XWK* mirror plane.

Figure 6 shows normal-emission EDC's from the (100) surface for the four different photon energies used. The vertical bars indicate calculated peak positions for the symmetry-allowed interband transitions $\Delta_1 \rightarrow \Delta_1$ and $\Delta_5 \rightarrow \Delta_1$. These results will also be discussed in Sec. V.

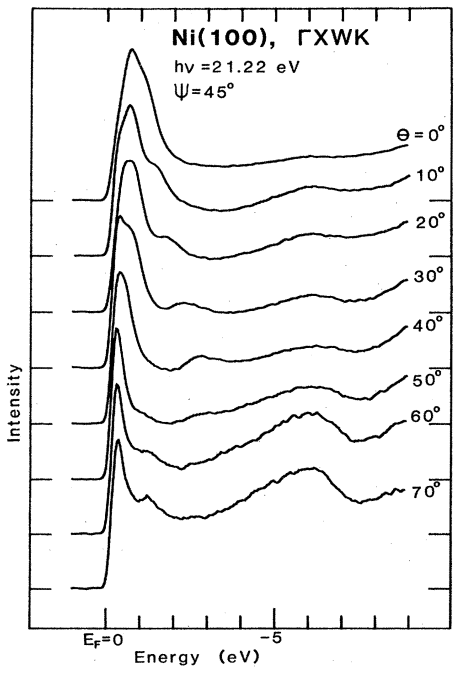

FIG. 5. Same as Fig. 2 but for Ni(100), Γ*XWK* mirror plane.

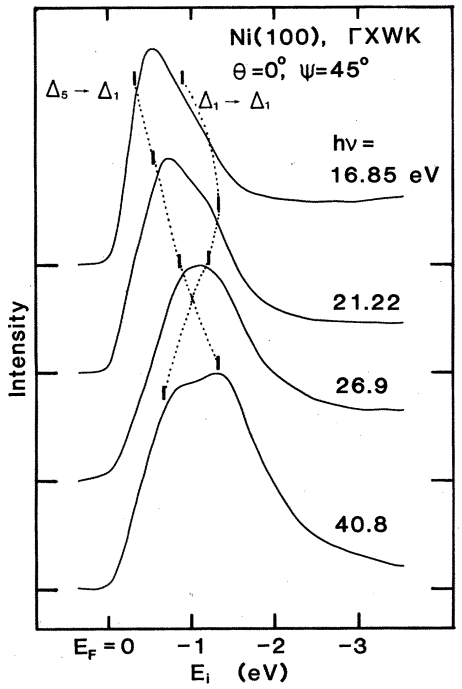

FIG. 6. Normal-emission EDC's from Ni(100) at four different photon energies. Photons were incident in the Γ*XWK* mirror plane. Positions for the symmetry-allowed transitions $\Delta_1 \rightarrow \Delta_1$ and $\Delta_5 \rightarrow \Delta_1$ have been calculated from our semiempirical band structure and are indicated by vertical bars.

IV. BAND-STRUCTURE DETERMINATION

In the photoemission process the energy, as well as the wave-vector component parallel to the surface, $\vec{k}_{||}$, is conserved. Since the perpendicular component $k_\perp$ is not conserved, a direct mapping of the electron-energy bands from photoemission data is not possible in general. Several methods have been developed to avoid this problem. The energy-coincidence method has been successfully applied mainly to the noble metals,[29,31,32] but a vast number of spectra at different detection angles and photon energies would be necessary in order to obtain a detailed picture of the band structure. The "symmetry method"[33] and the closely related "appearance-angle method"[34] exploit the rapid changes in the final-state energy and composition as Bragg planes are traversed. All these methods are ineffective in the sense that only a small part of the recorded data is actually used.

Another way is to assume a certain final-state band, e.g., a free-electron-like band, and calculate $k_\perp$ from that. This method has been used extensively in synchrotron-radiation investigations of noble and transition metals.[35,36] By recording EDC's normal to a low-index surface in a range of photon energies, the valence-state bands along the corresponding symmetry line may be directly mapped out. The use of free-electron-like bands is justified since the final-state bands may become free-electron-like due to the damping of the excited electron.[29,37] Nevertheless, since the final-state dispersion is based on an assumption,

the result will remain uncertain. Critical points, revealed by extremal behavior, will, however, be determined accurately by this method.

In the present study we have used a semi-empirical approach:[38] the systematic fitting of an interpolation scheme to the experimental data. We have used the combined interpolation scheme of Hodges, Ehrenreich, and Lang,[39] where the wave functions are expanded in a basis set consisting of four "orthogonalized plane waves" and five d states. The matrix elements constituting the secular equation are parametrized so that the resulting band structure depends on 15 parameters. The scheme was modified by use of symmetrizing factors of Smith and Mattheiss.[40] Actually the scheme is equivalent to that in Ref. 40 with the parameter S set equal to zero.

The first step of our analysis was to fit the parameters of the scheme to a number of experimentally-determined points of the band structure. The parameters subject to fitting were (notation in accordance with Ref. 40) α, V_{000}, R, B (B_t and B_e were assumed identical), E_0, A_1, A_2, A_3, A_4, A_5, and A_6. The reason for omitting V_{111} and V_{200} from the fit was that they are of great importance only above the Fermi level, where we lack experimental points of the band structure. The parameter S (representing nonlocal effects) that is omitted in our version of the scheme is not very important for the valence bands either. Finally, the crystal-field splitting Δ was found to be of minor importance too, and therefore set equal to zero.

As input data we used critical-point values from synchrotron-radiation investigations by Himpsel *et al.*[7] and by Eberhardt and Plummer.[9] The levels utilized were $(\Lambda_1)_{\min}$, $(\Delta_1)_{\min}$, Γ_{12}, Γ'_{25}, Γ'_1, L_2, L_3, X_2, and X_5. In cases of spin-split bands we used the spin-averaged value. In addition we used 11 points determined from our data by the energy-coincidence method. These latter points all belonged to the second and third lowest bands, and most of them were not located on symmetry lines. They were thus complementary to the critical-point data, giving a spread in $\vec{k}$ space that is favorable in order to obtain a good fit.

The next step was to compare the band structure obtained from the fitting procedure with our experimental results. This was done with aid of "structure plots," diagrams displaying the EDC peak positions E_p versus the emission angle θ. We calculated such structure plots using initial-state bands $E_i(\vec{k})$ from the interpolation scheme and free-electron-like final-state bands:

$$E_f(\vec{k})=\frac{\hbar^2k^2}{2m}+V_0 \ . \tag{1}$$

The resulting peak positions (on the initial-state energy scale) are then given by the E_i's satisfying the equations

$$E_i(\vec{k})+h\nu=\frac{\hbar^2k^2}{2m}+V_0 \ , \tag{2}$$

$$k_{||}^2=\frac{2m}{\hbar^2}[E_i(\vec{k})+h\nu-\phi]\sin^2\theta \ , \tag{3}$$

where $h\nu$ is the photon energy and ϕ is the work function. The extended-zone representation of $\vec{k}$ is presupposed. The inner potential V_0 is difficult to estimate accurately, so we chose just those values which gave the best agreement with the experimental results. Further, there may be deviations from the free-electron-like band close to the Bragg planes. The way to account for the approximations concerning the final state is to give it a certain width W, i.e., to relax Eq. (2) within some limits. The resulting structure plots then correspond to an inner potential ranging from $V_0-\frac{1}{2}W$ to $V_0+\frac{1}{2}W$. With enough broadening the free-electron-like band will enclose the true final-state band, and thus the true peak positions will be within the range of the broadened structure plot. The broadening of the final state is of some physical significance too, since it mimics one of the effects of damping in the final state.[41] The point is now that many of the structure-plot features remain narrow in spite of the final-state broadening. This means that these structures are rather insensitive to the final-state dispersion. By differentiation of Eqs. (2) and (3) we obtain

$$\left[\frac{\partial E_p}{\partial V_0}\right]_{\theta=\text{const}}=\frac{\partial E_i/\partial k_\perp}{(\partial E_i/\partial k_{||})(k_\perp/k_{||})\sin^2\theta+(\partial E_i/\partial k_\perp)\cos^2\theta-(\hbar^2k_\perp/m)} \ , \tag{4}$$

where E_p is the value of E_i that satisfies Eqs. (1) and (2), i.e., the EDC peak position. Since the $\vec{k}$-space gradients of the initial bands usually are small compared to the last term in the denominator, we can simplify to

$$\left[\frac{\partial E_p}{\partial V_0}\right]_{\theta=\text{const}}\approx\frac{m}{-\hbar^2k_\perp}\frac{\partial E_i}{\partial k_\perp} \ . \tag{5}$$

From these expressions it is obvious that the condition for obtaining narrow structure-plot features is that the initial bands are flat in the direction perpendicular to the surface.

Thus by comparing the calculated structure-plot features with the experimental data one can make systematic corrections in a refined fit of the interpolation-scheme parameters. By concentrating on the structures in which the calculations remain narrow, in spite of broadened final states, we are assured that the result is not sensitive to the approximations concerning the final states.

In our case we found that some of the calculated features, originating from the upper part of the d-band complex, were closer to the Fermi level than found experimentally. By repeating the fitting procedure with adjusted values of Γ_{12}, Γ'_{25}, and X_2 (lowered 0.15 eV relative to the first fit) we arrived at a band structure that gave good overall agreement between calculated and experimental structure plots. These plots are shown in Figs. 7–13. In Fig. 7 the experimental peak dispersions are compared

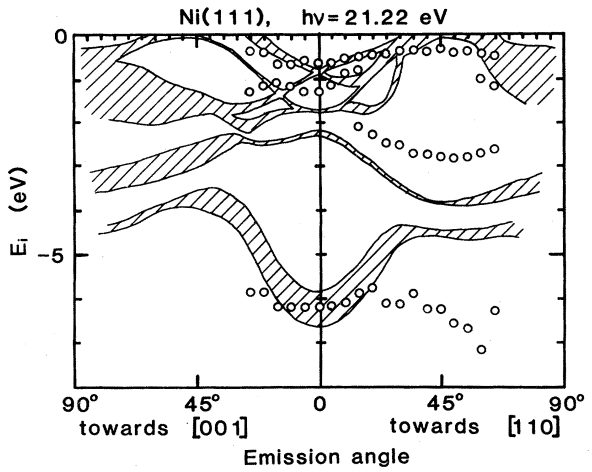

FIG. 7. Structure plot for mirror plane emission from the Ni(111) surface at photon energy $h\nu=21.22$ eV. Circles: experimental peak positions. Cross-hatched areas: peak positions calculated from the *ab initio* band structure of Moruzzi *et al.* (Ref. 42) with final-state broadening $W=4$ eV.

with a structure plot calculated from the theoretical band structure of Moruzzi, Janak, and Williams.[42] In all calculations the final-state broadening was 4 eV. The inner potential was -4 and -6 eV in the plots corresponding to 21.22- and 16.85-eV photon energy, respectively. The difference in the inner potential is an artifact due to the final-state approximation; the first value gives the best agreement with the actual final-state band in the energy range of interest at $h\nu=21.22$ eV, the second analogously at 16.85-eV photon energy.

The semiempirical band structure so obtained and the structure plots will be further discussed in the next section. The parameter values from the refined fit are listed in Table I.

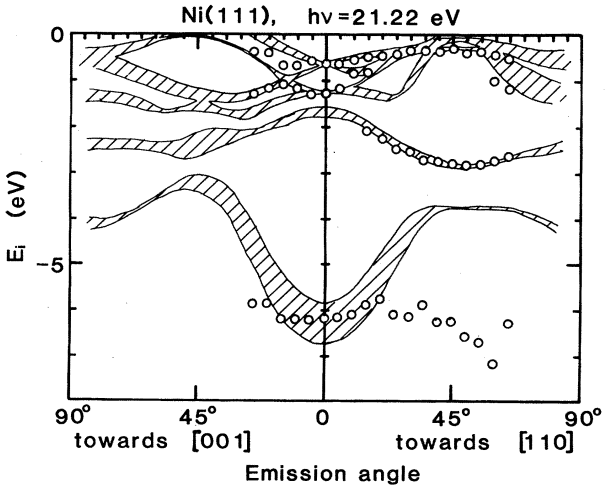

FIG. 8. Structure plot for mirror plane emission from the Ni(111) surface at photon energy $h\nu=21.22$ eV. Circles: experimental peak positions. Cross-hatched areas: peak positions calculated from our semiempirical band structure with final-state broadening $W=4$ eV.

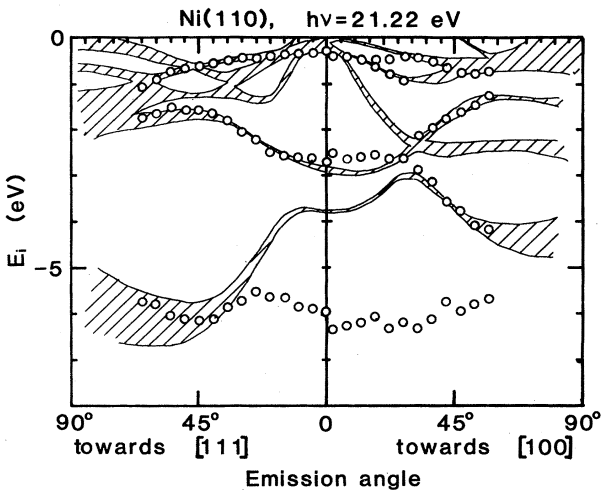

FIG. 9. Same as for Fig. 8 but from the Ni(110) surface.

V. DISCUSSION

We will now discuss the consistency of the experimental data with the semiempirical band structure. From Figs. 7 and 8 it is obvious that the semiempirical band structure is in far better agreement with the experimental results than the band structure calculated from first principles. With a few exceptions the calculated structure plots in Figs. 8—13 are in good agreement with the experimental points. Close to the Fermi level, experimental points in some cases (see Figs. 8, 9, 12, and 13) are found in the space between two predicted structures. This indicates that there actually are two peaks, but that they are too close to be resolved. The same problem is illustrated in Fig. 6 where the normal-emission EDC's of the (100) surface at four different energies are compared with peak positions predicted from the semiempirical band structure, and a free-electron-like final-state band with $V_0=-4$ eV. Ignoring spin-orbit interactions we expect from symmetry considerations[43] contributions only from initial-state

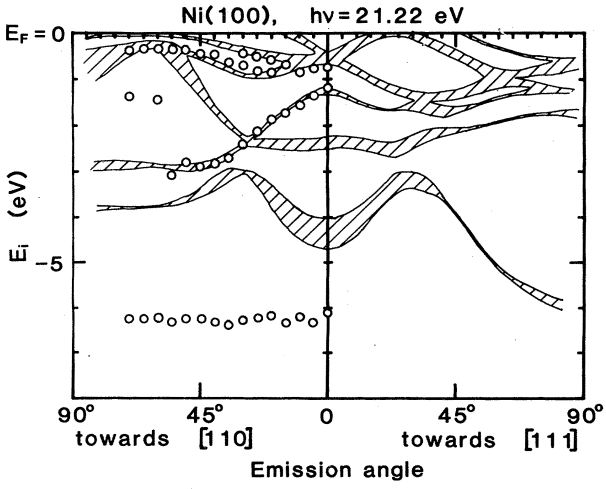

FIG. 10. Same as for Fig. 8 but from the Ni(100) surface.

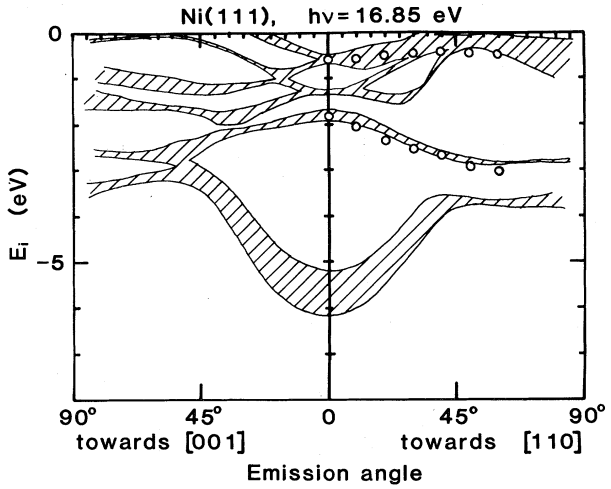

FIG. 11. Same as for Fig. 8 but with photon energy $h\nu=16.85$ eV.

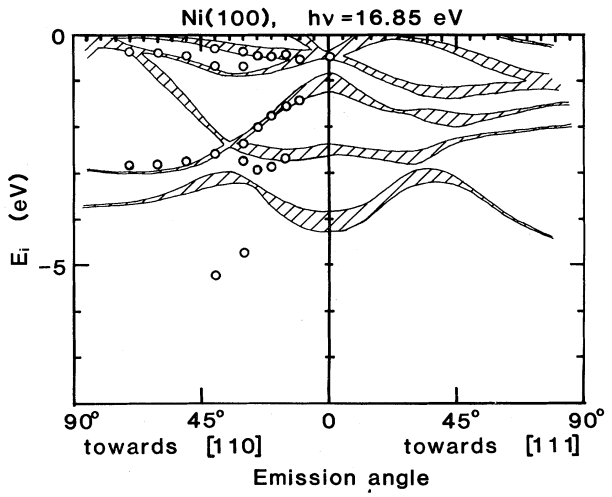

FIG. 13. Same as for Fig. 10 but with photon energy $h\nu=16.85$ eV.

bands of symmetries Δ_1 (p-polarized light) and Δ_5 (s-polarized light). Presented this way the connection is striking, but without the hints given by the calculated positions the compound nature of the peaks is clearly visible only in the EDC's obtained at $h\nu=21.22$ and 40.8 eV. Thus, in a situation of this kind, access to polarized radiation would be advantageous. Another complication is the Fermi-edge cutoff that may distort the peak shape, with erroneous values of the peak position as a consequence. Since we have not been able to resolve exchange splitting of peaks, our experimental peak positions correspond to the average positions in cases where both minority- and majority-spin bands are occupied. Going to an emission angle where the minority-spin band is cut off by the Fermi edge we can expect to obtain a peak position representing only the majority band. Thus close to the Fermi level the peak dispersion may become virtually diminished.

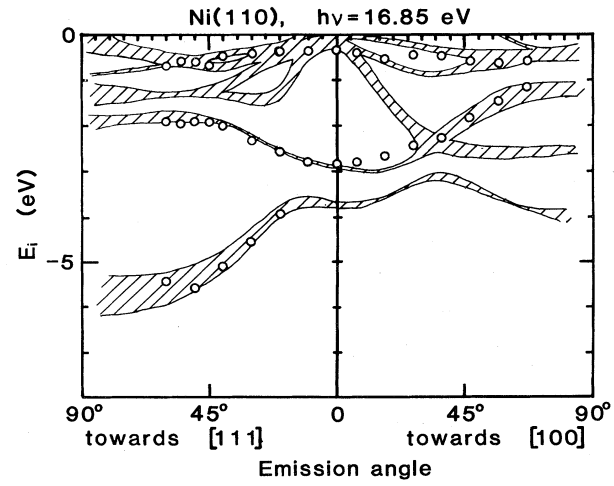

FIG. 12. Same as for Fig. 9 but with photon energy $h\nu=16.85$ eV.

Since input data from measurements resolving exchange splitting[7,9] close to the Fermi level were used in the interpolation scheme fit, we expect the interpolated band structure to be representative of paramagnetic bands, in spite of these effects. Also, the occurrence of surface states may complicate the interpretation of Ni EDC's. Surface states just below E_F have been reported for the (111) and (100) surfaces of Ni.[44–46] Of these the sp-like surface state on Ni(111) is characterized by a photoionization cross section rapidly decreasing with increasing photon energy.[44] At the photon energies used in our measurements, we do not expect emission from this surface state to influence our interpretation in terms of bulk state transitions. The magnetic surface state at the (100) surface may, however, be more troublesome since it is reported to contribute to the photoemission in a large range of photon energies and emission angles.[45,46] In our measurement it is not resolved, but it may cause a virtual shift of the nearest d-band peak. However, our band-structure determination does not rely on the (100) surface results close to E_F. As the calculated and experimental structure plots for the (100) surface (Figs. 10 and 13) do not show any

TABLE I. Interpolation-scheme parameters for the semiempirical Ni band structure. Notations and symmetrizing factors are in accordance with Smith and Mattheis (Ref. 40). Energies are in Ry with zero at the Fermi level, wave vectors are in units of $(2\pi/a)\times\frac{1}{12}$ (ΓX corresponds to 12 units).

α	0.0062	A_1	0.018 55
V_{000}	−0.650	A_2	0.006 64
V_{111}[a]	0.087 9	A_3	0.007 80
V_{200}[a]	0.109 5	A_4	0.010 88
R	0.239 3	A_5	0.001 59
B[b]	1.164 1	A_6	0.010 26
E_0	−0.077 19	Δ[a]	0

[a]Not included in the fitting process.
[b]B_t and B_e are taken equal.

large discrepancies close to E_F, we conclude that the disturbances due to unresolved surface states are small in this case.

Apart from discrepancies that can be blamed on unresolved multiple structures, there are structures in Fig. 10 (at $\theta=60°-70°$, $E_i\approx-1.4$ eV) and in Fig. 13 (at $\theta=30°-40°$, $E_i\approx-5$ eV) that may be attributed to "secondary cone emission."[47] The only remaining serious deviation from the calculated structure plots is the weak and broad structure at $E\approx-6$ eV that is clearly visible in all EDC's measured at $h\nu=21.22$ eV. From Figs. 8–10 it is obvious that this structure is not consistent with direct ($\vec{k}$ conserving) transitions. It may be identified with the 6-eV satellite mentioned in Section I. The picture is complicated by the fact that several adsorbed species (e.g., oxygen) give rise to structures at about the same energy. We cannot exclude the possibility that the structure in question is due to small amounts of oxygen or other contaminants that resisted the sputtering and annealing treatments. It is of course also possible that a combination of many-body effects and contaminants are responsible for the appearance of the structure. In some experimental configurations additional contributions due to direct transitions are possible. This may partially explain the dispersion observed around $\theta=45°$ in Fig. 9.

In Fig. 14(a) the semiempirical band structure is compared with the experimental data of Himpsel, Knapp, and Eastman[7] (HKE) and of Eberhardt and Plummer[9] (EP). The agreement is reasonably good, but there are differences that deserve some discussion.

Firstly, the experimental bands of HKE seem to be "repelled" from the zone boundaries at L and X compared to our semiempirical bands. Since their results are obtained from normal-emission measurements assuming a certain final band, the determination of $k_\perp$ is highly sensitive to the choice of the final bands. A shift of about 2 eV of the final band would be enough to yield excellent agreement with our results. Thus our data are fully consistent with those of HKE.

Secondly, the agreement with the critical points determined by EP is less satisfying. Several of their points are 0.2–0.4 eV higher in energy than in our results. This may be to some extent due to differences in the Fermi-level determination. The X_2 level is, however, nearly 0.6 eV lower in energy than ours. This is clearly inconsistent with our results, as well as those of Heimann *et al.*,[48] as will be seen in the following.

From Fig. 1 of Ref. 9 we can see that the photon energies we have used mostly (16.85 and 21.22 eV) give access to the $\vec{k}$-space region close to the X point. Since this makes us less dependent on the performance of the interpolation scheme, we expect the bands close to X to be particularly accurately determined by our method. Consider in Fig. 9 the second structure from above as θ ranges from 0 to 30° in the ΓXWK plane. The measured structure is in excellent agreement with the calculated structure, whose independence of the final-state band is indicated by its narrowness. This structure originates from a band that is connected to X_2, and as θ goes to zero we are getting very close to it. To combine the critical-point energy of EP with our data would demand an unrealistic deformation of the initial band. Analogously it can be said about the lowest band that the agreement of measurements and calculations seen in Figs. 9 and 12 is supporting our result for X_1. The somewhat higher energy found by EP can, apart from the uncertainty in the Fermi energy, be due to emission from X_3 that is not completely removed by the selection rules (due to finite angle resolu-

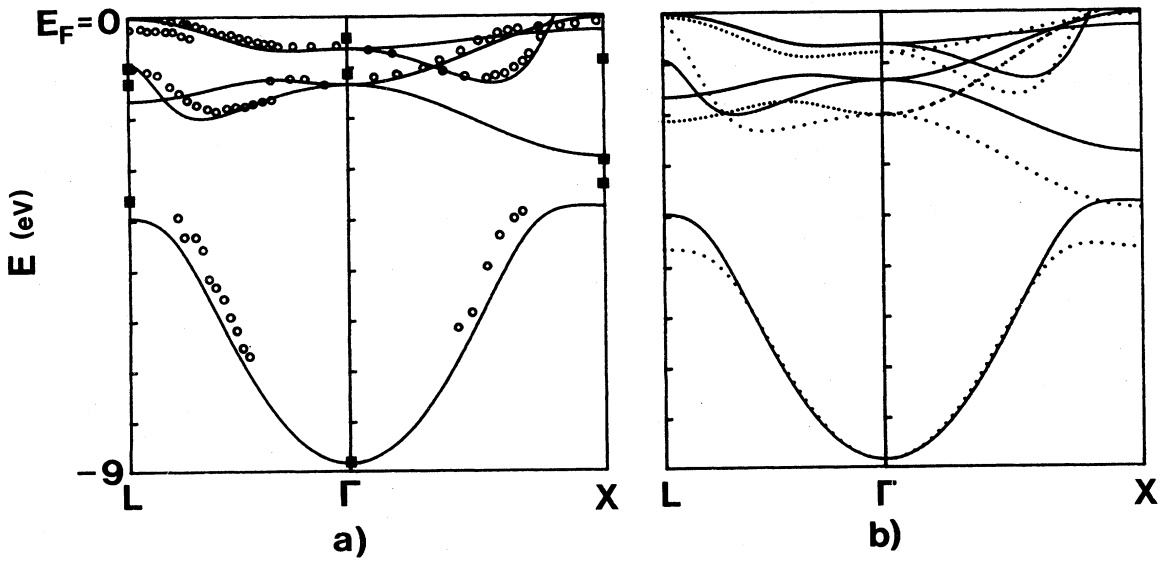

FIG. 14. Comparison of the semiempirical band structure of Ni (solid line) with (a) the bands mapped by Himpsel *et al.* (Ref. 7, circles), and critical points determined by Eberhardt and Plummer (Ref. 9, closed squares), and (b) the bands calculated by Moruzzi *et al.* (Ref. 42, dotted lines).

tion, etc.). The corresponding levels at L are not accessible with our photon energies, so we have to rely more on the ability of the interpolation scheme in that case. Compared to the calculated bands of Moruzzi *et al.*[42] [see Fig. 14(b)] our d-band width is 30% narrower, in good agreement with Refs. 6, 7, and 9.

Smith *et al.*[49] have recently published an empirical band structure obtained by adjusting three parameters in their exchange-split interpolation scheme originally fitted to a first-principles augmented-plane-wave calculation. Their results are in good agreement with ours, in spite of the difference in the number of constraints. This agreement provides strong support to the idea that the discrepancy between measured and calculated band structures of Ni is mainly a question of d-band position and width, while the band shape is not principally different.

ACKNOWLEDGMENTS

We wish to thank N. Dahlbäck for valuable discussions and assistance. Financial support from the Swedish Natural Science Research Council is also gratefully acknowledged.

[1]D. E. Eastman, in *Electron Spectroscopy,* edited by D. A. Shirley (North-Holland, Amsterdam, 1972), p. 487.
[2]C. S. Fadley and D. A. Shirley, in *Electronic Density of States,* edited by L. H. Bennet [Natl. Bur. Stand. (U.S.), Spec. Publ. 232] (U.S. GPO, Washington, D.C., 1971), p. 163.
[3]S. Hüfner, G. K. Wertheim, N. V. Smith, and M. M. Traum, Solid State Commun. **11**, 323 (1972).
[4]R. J. Smith, J. Anderson, J. Hermanson, and G. J. Lapeyre, Solid State Commun. **21**, 459 (1977).
[5]C. Guillot, Y. Ballu, J. Paigne, J. Lecante, K. P. Jain, P. Thiry, R. Pinchaux, Y. Petroff, and L. M. Falicov, Phys. Rev. Lett. **39**, 1632 (1977).
[6]D. E. Eastman, F. J. Himpsel, and J. A. Knapp, Phys. Rev. Lett. **40**, 1514 (1978).
[7]F. J. Himpsel, J. A. Knapp, and D. E. Eastman, Phys. Rev. B **19**, 2919 (1979).
[8]M. M. Traum, N. V. Smith, H. H. Farrel, D. P. Woodruff, and D. Norman, Phys. Rev. B **20**, 4008 (1979).
[9]W. Eberhardt and E. W. Plummer, Phys. Rev. B **21**, 3245 (1980).
[10]J. Barth, G. Kalkoffen, and C. Kunz, Phys. Lett. **74A**, 360 (1979).
[11]R. Clauberg , W. Gudat, E. Kisker, E. Kuhlmann, and G. M. Rothberg, Phys. Rev. Lett. **47**, 1314 (1981).
[12]D. R. Penn, Phys. Rev. Lett. **42**, 921 (1979).
[13]L. A. Feldkamp and L. C. Davis, Phys. Rev. Lett. **43**, 151 (1979).
[14]M. Iwan, F. J. Himpel, and D. E. Eastman, Phys. Rev. Lett. **43**, 1829 (1979).
[15]G. Treglia, F. Ducastelle, and D. Spanjaard, Phys. Rev. B **21**, 3729 (1980).
[16]L. C. Davis and L. A. Feldkamp, Solid State Commun. **34**, 141 (1980).
[17]A. Liebsch, Phys. Rev. Lett. **43**, 1431 (1979); Phys. Rev. B **23**, 5203 (1981).
[18]S. M. Girvin and D. R. Penn, J. Appl. Phys. **52**, 1650 (1981).
[19]G. Treglia, F. Ducastelle, and D. Spanjaard, J. Phys. (Paris) **43**, 341 (1982).
[20]S.-J. Oh, J. W. Allen, I. Lindau, and J. C. Mikkelsen, Phys. Rev. B **26**, 4845 (1982).
[21]L. Kleinman, Phys. Rev. B **19**, 1295 (1979); **22**, 468 (1980) [reply: W. Eberhardt and E. W. Plummer, Phys. Rev. B **22**, 6470 (1980)]; **22**, 6471 (1980) [reply: G. Treglia, F. Ducastelle, and D. Spanjaard, Phys. Rev. B **22**, 6472 (1980)].
[22]L. Kleinman and K. Mednick, Phys. Rev. B **24**, 6880 (1981).
[23]J. Kanski, P. O. Nilsson, and C. G. Larsson, Solid State Commun. **35**, 397 (1980).
[24]P. O. Nilsson, J. Kanski, and C. G. Larsson, in Proceedings of the VI International Conference on Vacuum Radiation Physics, Charlottesville, 1980 (unpublished).
[25]P. O. Nilsson, J. Kanski, and C. G. Larsson, Solid State Commun. **36**, 111 (1980).
[26]P. O. Nilsson, C. G. Larsson, and W. Eberhardt, Phys. Rev. B **24**, 1739 (1981).
[27]H. A. Padmore, C. Norris, G. C. Smith, C. G. Larsson, and D. Norman, J. Phys. C **15**, L155 (1982).
[28]V. I. Ansimov, M. I. Katsnelson, E. Z. Kurmaev, A. I. Liechtenstein, and V. A. Gubanov, Solid State Commun. **40**, 927 (1981).
[29]P. O. Nilsson and N. Dahlbäck, Solid State Commun. **29**, 303 (1979).
[30]E. O. Kane, Phys. Rev. Lett. **12**, 97 (1964).
[31]P. Heimann, H. Miosga, and H. Neddermeyer, Solid State Commun. **29**, 463 (1979).
[32]R. Courths, V. Bachelier, and S. Hüfner, Solid State Commun. **38**, 887 (1981).
[33]E. Dietz and D. E. Eastman, Phys. Rev. Lett. **41**, 1674 (1978).
[34]N. E. Christensen, Solid State Commun. **38**, 309 (1981).
[35]Y. Petroff and P. Thiry, Appl. Opt. **19**, 3957 (1980).
[36]F. J. Himpsel, Appl. Opt. **19**, 3964 (1980).
[37]D. W. Jepsen, F. J. Himpsel, and D. E. Eastman, Phys. Rev. B **26**, 4039 (1982).
[38]H. Mårtensson and P. O. Nilsson, Phys. Scr. T **4**, 152 (1983).
[39]L. Hodges, H. Ehrenreich, and N. D. Lang, Phys. Rev. **152**, 505 (1966).
[40]N. V. Smith and L. F. Mattheiss, Phys. Rev. B **9**, 1341 (1974).
[41]J. A. Knapp, F. J. Himpsel, and D. E. Eastman, Phys. Rev. B **19**, 4952 (1979).
[42]V. L. Moruzzi, J. F. Janak, and A. R. Williams, *Calculated Electronic Properties of Metals* (Pergamon, New York, 1978).
[43]W. Eberhardt and F. J. Himpsel, Phys. Rev. B **21**, 5572 (1980).
[44]F. J. Himpsel and D. E. Eastman, Phys. Rev. Lett. **41**, 507 (1978).
[45]E. W. Plummer and W. Eberhardt, Phys. Rev. B **20**, 1444 (1979).
[46]L. Erskine, Phys. Rev. Lett. **45**, 1446 (1980).
[47]G. D. Mahan, Phys. Rev. B **2**, 4334 (1970).
[48]P. Heimann, F. J. Himpsel, and D. E. Eastman, Solid State Commun. **39**, 219 (1981).
[49]N. V. Smith, R. Lässer, and S. Chiang, Phys. Rev. B **25**, 793 (1982).